JACS
JOURNAL OF THE AMERICAN CHEMICAL SOCIETY
Article
pubs.acs.org/JACS

Formation of Curvature Subunit of Carbon in Combustion

Xin-Zhou Wu, Yang-Rong Yao, Miao-Miao Chen, Han-Rui Tian, Jun Xiao, Yun-Yan Xu, Min-Song Lin, Laura Abella, Cheng-Bo Tian, Cong-Li Gao, Qianyan Zhang,* Su-Yuan Xie,* Rong-Bin Huang, and Lan-Sun Zheng

State Key Lab for Physical Chemistry of Solid Surfaces, iChEM (Collaborative Innovation Center of Chemistry for Energy Materials), Department of Chemistry, College of Chemistry and Chemical Engineering, Xiamen University, Xiamen 361005, China

Ⓢ *Supporting Information*

ABSTRACT: Curvature prevalently exists in the world of carbon materials (e.g., fullerenes, buckyl bowls, carbon nanotubes, and onions), but traditional C2-addition mechanisms fail to elucidate the mechanism responsible for the formation of carbon curvature starting from a pentagonal carbon ring in currently available chemical-physical processes such as combustion. Here, we show a complete series of nascent pentagon-incorporating C_5−C_{18} that are online produced in the flame of acetylene−cyclopentadiene−oxygen and in situ captured by C_{60} or trapped as polycyclic aromatic hydrocarbons for clarifying the growth of the curved subunit of $C_{20}H_{10}$. A mechanism regarding C1-substitution and C2-addition has been proposed for understanding the formation of curvature in carbon materials, as exemplified by the typical curved molecule containing a single pentagon completely surrounded by five hexagons. The present mechanism, supported by the intermediates characterized by X-ray crystallography as well as NMR, has been experimentally validated for the rational synthesis of curved molecule in the commercially useful combustion process.

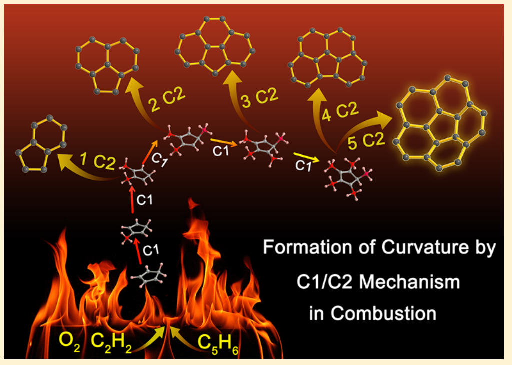

■ INTRODUCTION

In the last 30 years, scientists have shown favoritism for synthetic carbon allotropes in nanoscale, for example, fullerenes,[1] carbon nanotubes,[2] and graphenes.[3,4] The basic building blocks for these nanocarbons include the carbon frameworks of hexagon (for planarity) and pentagon (for curvature).[5] Synthesized by unclassical chemical-physical processes such as combustion,[6] as well as arc-discharge,[7] pyrolysis,[8] microwave plasma,[9] laser ablation,[1] glow discharge,[10] and chemical vapor deposition,[11] typical products of nanocarbons unavoidably incorporate structural curvature in a "random" yield under relatively extreme conditions. Specifically, the smallest curved subunit, C_{20} containing a single pentagon completely surrounded by five hexagons, prevalently exists in the form of such as $C_{20}H_{10}$, a stable molecule formally named as dibenzo[*ghi*,*mno*]fluoranthene and traditionally as corannulene or buckyl bowl, that has been chemically synthesized as early as 1966.[12] C2-addition mechanisms,[13−17] in which the C2 is the abbreviated form of the species containing two carbon atoms, are currently available for interpreting the formation of various nanocarbons. Although the C2-addition mechanisms are normally valid for planar structures, they are unable to reasonably interpret the prevalence of curvature in the products of the chemical-physical processes such as combustion. The mechanism responsible for the prevalent curvature originating from the pentagon, therefore, remains a mystery due to the absence of experimental evidence.

According to kinetic predictions and experimental measurements in the gas phase using molecular-beam mass spectrometry (MBMS) technology, the species containing a single carbon atom (C1 species) are abundant in the flame of hydrocarbons.[18−22] However, the C1 species, normally existed as radicals of hydrocarbons, have long been underrated in explaining nanocarbons growth. The main reasons for such an overlook might come from the fact that available nanocarbons contain basically an even number of carbon atoms. In addition, C1 species itself is extremely elusive, and rare experimental evidence supports C1 substitution involved in the chemical-physical processes.

Herein, we performed an experiment of acetylene−cyclopentadiene−oxygen combustion, applicable for the synthesis of curved nanocarbons and other carbonaceous particles, to search for the intermediates of curved molecules starting from cyclopentadiene. A series of methyl-substituted cyclopentadienyl (Cp) species have been captured in situ by nascent C_{60} in the forms of C_{60}(Cp), C_{60}(Cp)(CH_3), C_{60}(Cp)$(CH_3)_2$, C_{60}O(Cp)$(CH_3)_2$, C_{60}(Cp)$(CH_3)_3$, and C_{60}(Cp)$(CH_3)_4$ to establish the methyl-substituted Cp species as intermediates produced via a sequential C1 substitution from the original cyclopentadiene ring in the acetylene-cyclopentadiene-oxygen flame. Additionally, a series of single-pentagon-containing polycyclic aromatic hydrocarbons (PAHs) including acenaph-

Received: May 12, 2016
Published: July 5, 2016

 © 2016 American Chemical Society

DOI: 10.1021/jacs.6b04898
J. Am. Chem. Soc. 2016, 138, 9629−9633

thylene ($C_{12}H_8$), 4*H*-cyclopenta[*def*]phenanthrene ($C_{15}H_{10}$), benzo[*ghi*]fluoranthene ($C_{18}H_{10}$), and curved corannulene ($C_{20}H_{10}$) have been separated by high performance liquid chromatography (HPLC) and identified by nuclear magnetic resonance (NMR) or X-ray crystallography in the soot of the acetylene-cyclopentadiene-oxygen flame. All of these compounds (shown in Figure 1) constitute a complete series of

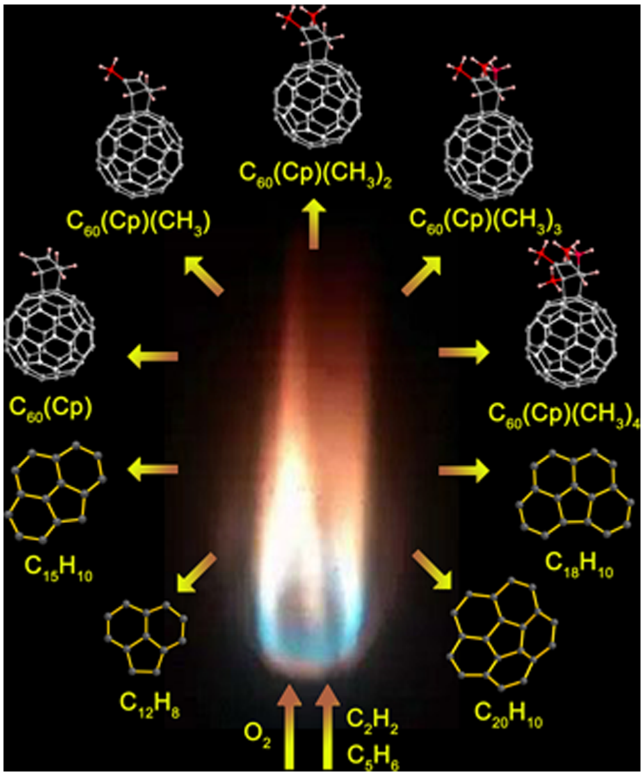

Figure 1. Illustration of the identified single-pentagon-containing PAHs and intermediates captured by C_{60} in the soot of the acetylene−cyclopentadiene−oxygen flame.

intermediates in the prerequisite chain from C_5 to C_{18} to establish a C1-substitution and C2-addition mechanism, that is, the C1/C2 mechanism, responsible for the curvature formation in the basic curved molecule. Furthermore, the proposed C1/C2 mechanism has shown validity for promoting combustion production of curved C_{20} subunit starting from selected C1/C2 reactants.

■ EXPERIMENTAL SECTION

The soot was synthesized by a low-pressure acetylene−cyclopentadiene−oxygen diffusion combustion method.[23] The diffusion flame, burned with mixture of reactants of oxygen, acetylene, and vaporous cyclopentadiene at the flow rate of 0.55, 1.10, and 1.20 L/min, respectively, was stabilized under a pressure of 20 Torr in a steel chamber. The soot, in a yield of ~5 g/h, was collected.

The crude toluene-extracting solutions of the soot are very complex and typically contain lots of PAHs, fullerenes, and fullerene derivatives. Preparative separation was conducted by multistep HPLC on four HPLC columns (pyrenebutyric acid, Buckyprep, 5PBB, and 5NPE) alternately in a Shimadzu LC-6AD HPLC instrument at room temperature, whereas chromatographic analysis was performed by HPLC-APCI-MS/UV−vis using an Agilent 1200 series instrument coupled with a Bruker Esquire HCT mass spectrometer interfaced by APCI (atmospheric pressure chemical ionization) source. The column used for chromatographic analysis was a Supelco Discovery C18 (i.d. 4.6 × 250 mm) column. A gradient elution of methanol−ethanol−cyclohexane was taken at a flow rate of 0.8 mL/min. The procedures for both preparative isolation and HPLC-APCI-MS/UV−vis analysis are detailed in the Supporting Information.

The diffraction data of $C_{60}O(Cp)\ (CH_3)_2$ were collected on an Agilent Technologies SuperNova system with Cu Kα radiation (λ = 1.54178 Å) at 100 K. The data were processed using CrysAlis^{Pro}.[24] The structure was solved and refined using full-matrix least-squares based on F^2 with programs SHELXS-2015 and SHELXL-2015[25] within Olex2.[26]

■ RESULTS AND DISCUSSION

HPLC-APCI-MS/UV−Vis Analysis and HPLC Separation of Toluene-Soluble Products. The HPLC chromatogram of the toluene-soluble products extracted from the combustion soot was determined by mass spectrometry (MS) in a C18 column with methanol−ethanol−cyclohexane as eluent (Table S1). At the retention time of 86−87 min, a series of MS signals of 786, 800, 814, 828, 830, and 842 atomic mass units (amu) were acquired in corresponding MS with atmosphere pressure chemical ionization (APCI) as the ion source (Figure 2 and

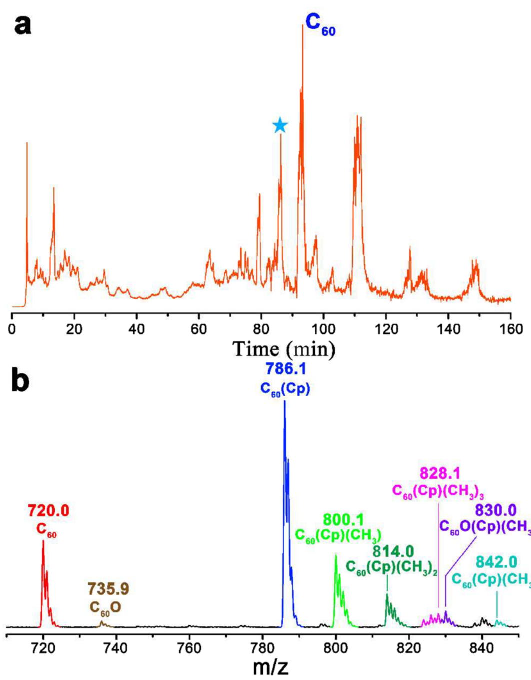

Figure 2. (a) HPLC chromatogram of the toluene-extracted soot products. (b) APCI-MS for the components at the retention time of 86−87 min.

Figures S1−S6). Obviously, the signals of 786, 800, 814, 828, and 842 amu can be identified as a class of homologous derivatives of C_{60} with difference of 14 amu, such as $C_{60}(Cp)$, $C_{60}(Cp)(CH_3)$, $C_{60}(Cp)(CH_3)_2$, $C_{60}(Cp)(CH_3)_3$, and $C_{60}(Cp)(CH_3)_4$, resulting from the H atom of cyclopentadiene (C_5H_6) replaced by methyl group in turn, and the signal of 830 amu can be assigned to the mono-oxidation product of $C_{60}(Cp)(CH_3)_2$. All of these C_{60} derivatives, separated by HPLC (Figures S7−S16), can be considered as the intermediates captured by fullerene cages.[27] Certainly there are more PAHs products in the soot, but most of the PAHs are hard to detect directly by APCI-MS.[28] Among them, $C_{12}H_8$, $C_{15}H_{10}$, and $C_{18}H_{10}$ were further separated by HPLC and structurally identified by NMR or X-ray crystallography (Figures S17−S23 and Table S2). Specifically, corannulene

DOI: 10.1021/jacs.6b04898
J. Am. Chem. Soc. 2016, 138, 9629−9633

$C_{20}H_{10}$ was confirmed by standard comparison experiment with analytical methods including HPLC and UV−vis spectrometric detection (Figures S24−S26 and Table S3).[14,29]

Crystallographic Identification of $C_{60}O(Cp)(CH_3)_2$. In the products of acetylene−cyclopentadiene−oxygen flame, $C_{60}O(Cp)(CH_3)_2$ has been identified by single-crystal X-ray diffraction as well as MS, IR, and UV−vis methods (Figures S27, S28). In cyclohexane solution of $C_{60}O(Cp)(CH_3)_2$, black-colored single crystals suitable for X-ray diffraction determination were grown by slow evaporation of solvent. The structure of $C_{60}O(Cp)(CH_3)_2$ identified by X-ray crystallography is shown in Figure 3 [CCDC 1458672 contains the supplementary crystallographic data for $C_{60}O(Cp)(CH_3)_2$]. Note that the molecule is intrinsically chiral but shown without enantioseparation.[30] Importantly, the geometric structures with the addition positions of addends of $Cp(CH_3)_2$ and oxygen have been identified unambiguously, which allows one to get insight into the mechanistic details for capture of the pentagon-involving intermediates by fullerene derivatization. As known, there are two types of C−C bonds, [6, 6] bond and [5, 6] bond, in the skeleton of I_h-C_{60}. Usually, the [6, 6] bond is shorter and exhibits chemical reactivity of a C═C double bond.[31] Thus, the $(Cp)(CH_3)_2$ specie is added to the reactive [6, 6] bond (C_1−C_2) on the C_{60} cage. Once the [6, 6] bond was attacked, the length of the bond (C_1−C_2) is elongated to 1.594(9) Å. In contrast, the bond length of adjacent [6, 6] has to shrink, rendering more double bond character.[32] Accordingly, the additional oxygen atom should exclusively be added to the adjacent [6, 6] bond (C_3−C_4) to form epoxide-like structure by an oxidative addition.

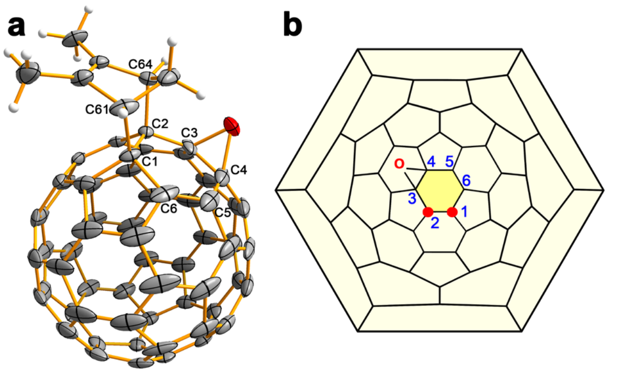

Figure 3. (a) Oak Ridge thermal ellipsoid plot (ORTEP) drawing with thermal ellipsoids at the 30% probability level. (b) Schlegel diagram of $C_{60}O(Cp)(CH_3)_2$ with the $(Cp)(CH_3)_2$ moiety bonded by red dots. Selected bond distances: C_1−C_{61}, 1.595(10) Å; C_2−C_{64}, 1.600(9) Å; C_1−C_2, 1.594(9) Å; C_3−C_4, 1.485(13) Å (Figure S29 and Table S4).

^{1}H NMR Characterization and Theoretical Calculation for $C_{60}(Cp)(CH_3)_n$ (n = 0−4). Macroscopic quantities of $C_{60}(Cp)(CH_3)_n$ (n = 0−3) were isolated for ^{1}H NMR identification (Figures S30−S33). As shown in Figure 4a, the ^{1}H NMR spectrum of $C_{60}(Cp)$ exhibits four groups of H. Integral ratios for the four kinds of protons are nearly 2:2:1:1. Among them, chemical shift of the H linking to double bond in the Cp ring is moved to low field (7.2 ppm) due to less of a shielding effect. The two hydrogen atoms on the mono carbon bridge are divided by 2.5 and 3.5 ppm, in which the signal of 2.5 ppm should be assignable to the H close to C_{60} because of the shielding effect. The ^{1}H−^{1}H COSY spectrum of $C_{60}(Cp)$ accords well with the proposed structure (Figures S34−S37).

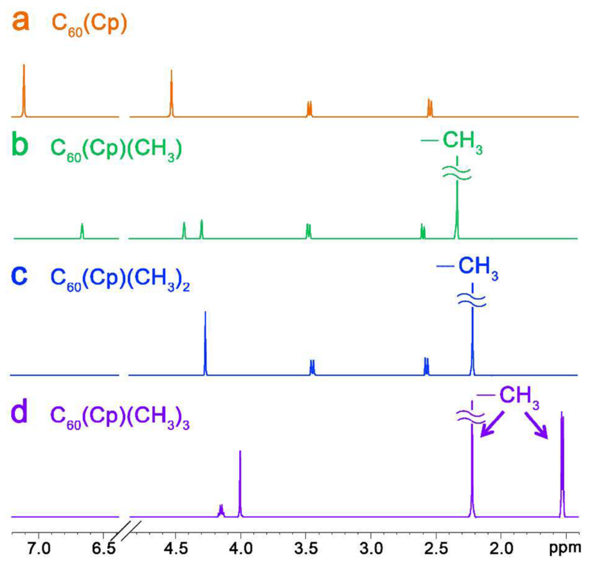

Figure 4. Diagram of ^{1}H NMR shifts for $C_{60}(Cp)$, $C_{60}(Cp)(CH_3)$, $C_{60}(Cp)(CH_3)_2$, and $C_{60}(Cp)(CH_3)_3$ adapted from experimental data (Figures S30−S33).

The correlation of two hydrogens at the mono carbon bridge is the strongest, and all of the other hydrogen atoms on adjacent carbons show good correlation with each other.

With the replacement of the methyl group, new signals come out at high field (1.0−2.5 ppm), and the protons located at low field decrease from two to one and even disappear as shown in Figure 4b,c. Apparently, the hydrogen atoms linking to double bonds are successively substituted by methyl groups resulting in mono- and dimethyl-substituted $C_{60}(Cp)$. Judging from the ^{1}H NMR spectrum of trimethyl-substituted $C_{60}(Cp)$ (Figure 4d), one of two hydrogens located at the mono carbon bridge is replaced by the third methyl group. The signal of H in the third substituted methyl group locates at high field around 1.5 ppm, while the chemical shift of the remained H on the mono carbon bridge moves to downfield (4.1 ppm) due to the effect of van der Waals force occurring as hydrogen atoms are congested with each other. The ^{1}H−^{1}H COSY spectrum of $C_{60}(Cp)(CH_3)_3$ also reveals a strong correlation between the H in the third methyl group and the H located at bridgehead carbon (Figure S37). Although the MS signal of the tetramethyl-substituted $C_{60}(Cp)$ was observed in the LC−MS spectrum, we failed to obtain enough sample to fulfill its ^{1}H NMR characterization. With the prediction of theoretical calculation, the fourth methyl group should link to one of the bridgehead carbons in the structure of $C_{60}(Cp)(CH_3)_4$, which is more favorable than the isomer with two methyl substituted at the mono carbon bridge in terms of relative energy (Figure S38). In addition, theoretical calculation for all four possible monomethyl-substituted $C_{60}(Cp)(CH_3)$ isomers is helpful for the explanation of the regioselectivity of methyl groups in $C_{60}(Cp)(CH_3)_n$ (n = 1−3), in accord with those revealed in the ^{1}H NMR spectra (Figure S39 and Table S5).

Mechanism Responsible for Curvature Formation in the Acetylene−Cyclopentadiene−Oxygen Flame. Much previous research has been devoted to understanding how chain reactions initiate in combustion of hydrocarbons, and how intermediate interactions dictate formation of the first aromatic compound with a six-membered ring.[33] In traditional C2-addition mechanisms,[13−17] large carbonaceous species are

DOI: 10.1021/jacs.6b04898
J. Am. Chem. Soc. 2016, 138, 9629−9633

supposed to grow from benzene with the first step reaction of H-abstraction to form aryl radical, and then two steps of C_2H_2-addition to aryl radical to form an ortho vinylic radical leading to naphthalene $C_{10}H_8$.[15] It is hard to undergo such an ortho regioselectivity to produce curved molecules like corannulene. The C2 mechanisms are unable to explain the formation of some PAHs containing an odd number of carbons, such as the $C_{15}H_{10}$ produced in the present combustion. On the basis of the identified structures in this work, shown in Scheme 1, the whole process of the corannulene-like curvature formation in the combustion can be assumed starting from pentagon (the five-membered ring in the reactant of cyclopentadiene), and then sequential steps of C1-substitution and C2-addition resulting in the obtained $C_{12}H_8$, $C_{15}H_{10}$, $C_{18}H_{10}$, and $C_{20}H_{10}$. Two steps of C1-substitution and one step of C2-addition form intermediate indene (C_9H_8), which has been detected in the flame of acetylene or cyclopentadiene (note that C_9H_8 is hard to be separated in the solid state by our chromatographic procedure, but it has been identified by gas chromatography-flame ionization detection[34] or MBMS, tunable synchrotron vacuum ultraviolet photoionization[21]). Further C1-substitution and C2-addition provide a series of representative products of $C_{12}H_8$, $C_{15}H_{10}$, $C_{18}H_{10}$, as well as the curved $C_{20}H_{10}$ (Scheme 1). Such a C1/C2 mechanism in combination with both C1-substitution and C2-addition makes the ortho regioselectivity no longer a wicked problem, and thereof provides a reasonable explanation for the formation of curvature subunit. Furthermore, all flat and curved PAHs including odd or even number of carbons can be accomplished with the proposed C1/C2 mechanism.

Scheme 1. Proposed Schematic Diagram for Curvature Subunit of C_{20} Formation by C1/C2 Mechanism

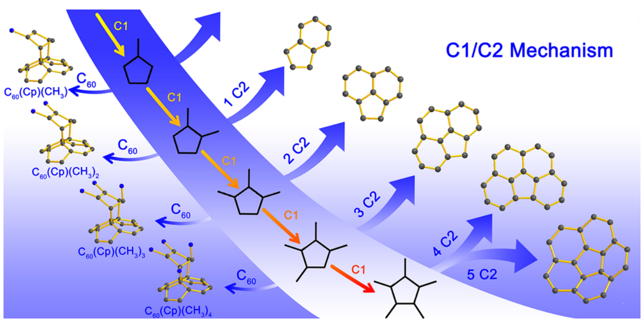

It is not surprising that some kinds of methyl species survive in the flame conditions to dictate the C1 substitution for the sequential formation of $C_{60}(Cp)(CH_3)_n$ (n = 1−4), because hydrocarbon fuels have been interpreted to decompose as smallest species in the initial step of combustion.[18] In the present work, specifically, C1 substitution is possibly derived from a contribution of extremely reactive methylene carbene species due, in part, to the involvement of acetylene. A possible mechanism for the formation of multiple methyl-substituted Cp species is shown in Scheme 2, exemplifying the growth of smaller carbon species based on C1-substitution in the present acetylene−cyclopentadiene−oxygen flame. First, acetylene and oxygen produce reactive methylene carbene species; the speed of this step reaction is fast according to the previous literature report.[35,36] The formed methylene carbene species then inserts into the cyclopentadiene molecule to give a monomethyl-substituted Cp species. Subsequently, repeated carbene insertions produce a series of Cp species of $(Cp)(CH_3)_2$, $(Cp)(CH_3)_3$, and $(Cp)(CH_3)_4$ subjected to capture by C_{60}.

Scheme 2. Exemplified Mechanism for the Formation of Methyl-Substituted Cp Species

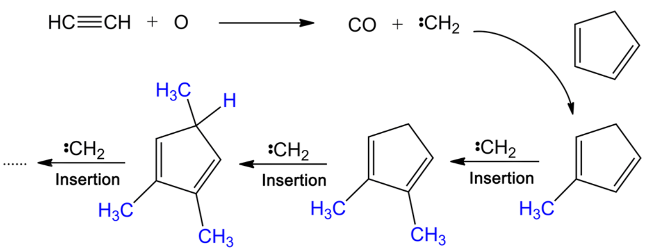

Obviously, addition of methane into the flame would increase the C1 species in the combustion process. To validate the importance of C1 in the formation of curvature, methane was added into the fuel-rich flames of acetylene−cyclopentadiene−oxygen in the conditions described in Table S6. As shown in Figure 5, an introduction of 1−2% methane is quite beneficial for improving the yield of $C_{20}H_{10}$. An acetylene−benzene−oxygen flame was performed for comparison, and cyclopentadiene was revealed more favorable for the formation of $C_{20}H_{10}$ than benzene. Therefore, the control experiment results reveal that cyclopentadiene, acetylene, and methane (partly representing C5, C2, and C1, respectively) play key roles in the formation of curvature subunit, which support the C1/C2 mechanism to some extent.

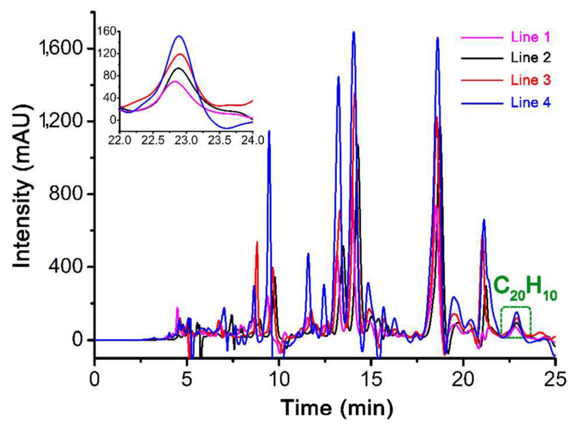

Figure 5. Quantitative HPLC analysis for the curvature of $C_{20}H_{10}$ deriving from different combustion flames. Line 1, acetylene−benzene−oxygen flame; line 2, acetylene−cyclopentadiene−oxygen flame; line 3, methane(1%)−acetylene(99%)−cyclopentadiene−oxygen flame; line 4, methane(2%)−acetylene(98%)−cyclopentadiene−oxygen flame.

■ CONCLUSION

The complete series of single-pentagon-containing compounds toward C_{20}, the basic subunit of curvature, were captured from acetylene−cyclopentadiene−oxygen flame. The compounds ranging from C_5 to C_{18} were unambiguously identified in the forms of $C_{60}(Cp)(CH_3)_n$ (n = 1−4), $C_{60}O(Cp)(CH_3)_2$, as well as $C_{12}H_8$, $C_{15}H_{10}$, and $C_{18}H_{10}$. Different from previously reported interpretations, a C1/C2 mechanism has thus been proposed for understanding of curvature formation in nanocarbon materials. As exemplified by $C_{20}H_{10}$, the proposed mechanism is validated for improving the yield of curved

DOI: 10.1021/jacs.6b04898
J. Am. Chem. Soc. 2016, 138, 9629−9633

molecules and thus expected for rational synthesis of other curved carbonaceous materials in the combustion of hydrocarbons.

■ ASSOCIATED CONTENT

Supporting Information

The Supporting Information is available free of charge on the ACS Publications website at DOI: 10.1021/jacs.6b04898.

Detailed experimental procedures and characterization data (PDF)

X-ray crystal data for $C_{60}O(Cp)(CH_3)_2$ (CIF)

■ AUTHOR INFORMATION

Corresponding Authors

*xmuzhangqy@xmu.edu.cn

*syxie@xmu.edu.cn

Notes

The authors declare no competing financial interest.

■ ACKNOWLEDGMENTS

The work was supported by the 973 Program of China (2014CB845601 and 2015CB932301) and the National Natural Science Foundation of China (U1205111, 21390390, 21301143, and 51572231).

■ REFERENCES

(1) Kroto, H. W.; Heath, J. R.; O'Brien, S. C.; Curl, R. F.; Smalley, R. E. *Nature* **1985**, *318*, 162−163.
(2) Iijima, S. *Nature* **1991**, *354*, 56−58.
(3) Novoselov, K. S.; Geim, A. K.; Morozov, S. V.; Jiang, D.; Zhang, Y.; Dubonos, S. V.; Grigorieva, I. V.; Firsov, A. A. *Science* **2004**, *306*, 666−669.
(4) Novoselov, K. S.; Jiang, D.; Schedin, F.; Booth, T. J.; Khotkevich, V. V.; Morozov, S. V.; Geim, A. K. *Proc. Natl. Acad. Sci. U. S. A.* **2005**, *102*, 10451−10453.
(5) Bettinger, H. F.; Yakobson, B. I.; Scuseria, G. E. *J. Am. Chem. Soc.* **2003**, *125*, 5572−5580.
(6) Howard, J. B.; McKinnon, J. T.; Makarovsky, Y.; Lafleur, A. L.; Johnson, M. E. *Nature* **1991**, *352*, 139−141.
(7) Kraetschmer, W.; Lamb, L. D.; Fostiropoulos, K.; Huffman, D. R. *Nature* **1990**, *347*, 354−358.
(8) Taylor, R.; Langley, G. J.; Kroto, H. W.; Walton, D. R. M. *Nature* **1993**, *366*, 728−731.
(9) Xie, S.-Y.; Huang, R.-B.; Yu, L.-J.; Ding, J.; Zheng, L.-S. *Appl. Phys. Lett.* **1999**, *75*, 2764−2766.
(10) Xie, S.-Y.; Huang, R.-B.; Chen, L.-H.; Huang, W.-J.; Zheng, L.-S. *Chem. Commun.* **1998**, 2045−2046.
(11) Li, W. Z.; Xie, S. S.; Qian, L. X.; Chang, B. H.; Zou, B. S.; Zhou, W. Y.; Zhao, R. A.; Wang, G. *Science* **1996**, *274*, 1701−1703.
(12) Barth, W. E.; Lawton, R. G. *J. Am. Chem. Soc.* **1966**, *88*, 380−381.
(13) Frenklach, M.; Wang, H. *Symp. (Int.) Combust., [Proc.]* **1991**, *23*, 1559−1566.
(14) Lafleur, A. L.; Howard, J. B.; Taghizadeh, K.; Plummer, E. F.; Scott, L. T.; Necula, A.; Swallow, K. C. *J. Phys. Chem.* **1996**, *100*, 17421−17428.
(15) Richter, H.; Howard, J. B. *Prog. Energy Combust. Sci.* **2000**, *26*, 565−608.
(16) Frenklach, M. *Phys. Chem. Chem. Phys.* **2002**, *4*, 2028−2037.
(17) Omidvarborna, H.; Kumar, A.; Kim, D.-S. *Renewable Sustainable Energy Rev.* **2015**, *48*, 635−647.
(18) Richter, H.; Howard, J. B. *Phys. Chem. Chem. Phys.* **2002**, *4*, 2038−2055.
(19) Hennessy, R. J.; Robinson, C.; Smith, D. B. *Symp. (Int.) Combust., [Proc.]* **1988**, *21*, 761−772.
(20) Bhargava, A.; Westmoreland, P. R. *Combust. Flame* **1998**, *113*, 333−347.
(21) Li, Y.; Zhang, L.; Tian, Z.; Yuan, T.; Zhang, K.; Yang, B.; Qi, F. *Proc. Combust. Inst.* **2009**, *32*, 1293−1300.
(22) Qi, F.; Yang, R.; Yang, B.; Huang, C.; Wei, L.; Wang, J.; Sheng, L.; Zhang, Y. *Rev. Sci. Instrum.* **2006**, *77*, 084101.
(23) Weng, Q.-H.; He, Q.; Liu, T.; Huang, H.-Y.; Chen, J.-H.; Gao, Z.-Y.; Xie, S.-Y.; Lu, X.; Huang, R.-B.; Zheng, L.-S. *J. Am. Chem. Soc.* **2010**, *132*, 15093−15095.
(24) *CrysAlisPro, Version 1.171.35.19*; Agilent Technologies Inc.: Santa Clara, CA, 2011.
(25) Sheldrick, G. M. *Acta Crystallogr., Sect. C: Struct. Chem.* **2015**, *71*, 3−8.
(26) Dolomanov, O. V.; Bourhis, L. J.; Gildea, R. J.; Howard, J. A. K.; Puschmann, H. *J. Appl. Crystallogr.* **2009**, *42*, 339−341.
(27) Weng, Q.-H.; He, Q.; Sun, D.; Huang, H.-Y.; Xie, S.-Y.; Lu, X.; Huang, R.-B.; Zheng, L.-S. *J. Phys. Chem. C* **2011**, *115*, 11016−11022.
(28) Gao, Z.-Y.; Jiang, W.-S.; Sun, D.; Xie, Y.; Chen, Z.-L.; Yu, L.-J.; Xie, S.-Y.; Huang, R.-B.; Zheng, L.-S. *Talanta* **2010**, *81*, 48−54.
(29) Lafleur, A. L.; Howard, J. B.; Marr, J. A.; Yadav, T. *J. Phys. Chem.* **1993**, *97*, 13539−13543.
(30) Liu, J. L.; Liu, W.; Huang, G. Z.; Tong, M. L. *Sci. Bull.* **2015**, *60*, 447−452.
(31) Diederich, F.; Thilgen, C. *Science* **1996**, *271*, 317−323.
(32) Chikama, A.; Fueno, H.; Fujimoto, H. *J. Phys. Chem.* **1995**, *99*, 8541−8549.
(33) Bittner, J. D.; Howard, J. B. *Symp. (Int.) Combust., [Proc.]* **1981**, *18*, 1105−1116.
(34) Butler, R. G.; Glassman, I. *Proc. Combust. Inst.* **2009**, *32*, 395−402.
(35) Fenimore, C. P.; Jones, G. W. *J. Chem. Phys.* **1963**, *39*, 1514−1518.
(36) Vinckier, C.; Schaekers, M.; Peeters, J. *J. Phys. Chem.* **1985**, *89*, 508−512.